International Journal of Advancements in Mechanical and Aeronautical Engineering– IJAMAE
Volume 2: Issue 1 [ISSN : 2372-4153]
Publication Date : 30 April, 2015

Bone Porosity Modeling and FE Simulation

Abdulaziz S. Al-Aboodi, Abdulrahman A. Al-Nasser

***Abstract*—Porosity in bone has many functions, which are decreasing the mass of bone relative to its volume, allow fluid to transfer through bones and give some ductility to the bone material. So that, the artificial bone should include porosity to imitate bone structure. To achieve the porosity functions on artificial bone many requirement should be consider such as material property and structure requirements. Researchers had modeled porosity by either regular or irregular shaped. Irregular shape has been modeled by copying several layers from natural pone CT scan images. Regular porous shape could be design by deferent shapes that confirm the porosity function requirement. The aim of this paper is to propose model that satisfy the function of porosity in real bone and attain the requirement on material and structure.**

***Keywords*— Bone, Porosity, Modelling, Finite Element**

I. Introduction

Porosity in bone takes different shapes and geometry in deferent bones depending on the bone function, place and other factors. Researchers introduced models of the bone porosity using different methods. Some of them by using different bone cross sectional images using CT-Scan then they exported them to image processing software to develop a 3D model that imitate the actual bone with irregular porosity geometry. Others tries to developed porous model with regular and symmetry geometry of porosity. The benefit of regular porosity geometry models is to include its variable dimensional parameters that could be modified to produce optimum parameters in respect of material mechanical properties. the porous shaped should have a capability to transmit fluid inside the porous material with uniform distribution. Introducing properties on material will change its mechanical properties. The most important mechanical properties are the yield strength and elastic modulus. Acharya et al [1] present a method to construct a simple and general site bond correlated 3D Hydraulic Pore Network model of hydraulic behavior of porous media for a wide range of permeability and porosity. Modelling porosity of biomaterials is critical for developing replacement bone tissues. Schroeder [2] et al uses this representation to develop an approach to modelling of porous, heterogeneous materials.

Abdulaziz S. Al-Aboodi
Engineering College / Qassim University
Saudi Arabia

Abdulrahman A. Al-Nasser
Buraydah Technical College
Saudi Arabia

Zeleniakienė et al [3] investigated the stresses of 2D and 3D Representative Volume Element of porous polymer material. They compare the two models and evaluate the differences between them in the cases of various porosity modes. Komlev et al [4] investigated a highly porous hydroxyapatite scaffolds before the implantation and after they were seeded within vitro expanded bone marrow stromal cells (BMSC) and implanted for various nombers of weeks in mice. Kujime et al[5] made a three-dimensional (3D) reconstruction of the microstructure of the lotus-type porous carbon steel using an image-based modelling to simulate the mechanical behavior using finite element method. Li [6] fabricated titanium alloy scaffolds using 3D fiber deposition. Then they analyzed them in vivo performance of the scaffolds with different structural properties. Shen et al [7] examined the deformation of a relatively low porosity of porous titanium using two-dimensional plane strain and three-dimensional finite element models to identify the accuracy and limitations of such simulations. Helgason et al [8] compare the results from subject-specific finite element analysis of a human femur to experimental measurements, using two different methods for assigning material properties to the FE models. Teoh et al [9] survey the literature in the area of bone material properties and Needle/bone interaction in the context of needle placement. Verges et al [10] described the methodology that they have designed to quantify the pores distribution in bone implants and the empirical results that they have obtained with CAD designed scaffolds, micro-CT and confocal microscopy data. They segmented the 3D images into three regions: exterior, bone and pore space. Next, they divide the pore space into pores and connection paths. Kou et al [11] presented an alternative approach to design irregular porous artifacts with controllable pore shapes and distributions without requiring any existing objects as prerequisites. Michailidis et al [12], [13] introduced and facilitating the establishment of a FEM model corresponding to a solid geometry of open-cell foams for simulating the material behavior in micro-tension. Voronov et al [14] investigated the shear stress distributions within Poly-L-lactic acid scaffolds via computation. Scaffolds used in this study are prepared via salt leeching with various geometric characteristics. High-resolution micro-computed tomography is used to obtain their 3D structure. Flow of osteogenic media through the scaffolds is modelled via lattice Boltzmann method. Zaretskiy et al [15] presented a finite element–finite volume simulation method for modelling single-phase fluid flow and solute transport in experimentally obtained 3D pore geometries. Park et al [16] designed and fabricated 3D plotting system and three types of scaffolds using a rapid prototyping technique. Podshivalov et al [17] describes a new alternative for individualized mechanical analysis of bone trabecular structure. Guillén et al [18] studied compressive behavior of bovine cancellous bone and three open-cell metallic foams using mechanical testing, micro-

focus computed tomography and finite element modelling. Spaggiari et al [19], [20] presented a combined finite-element and analysis of variance study of polymeric materials containing spherical and ellipsoidal voids. Ren et al [21] tested and evaluated mechanical properties changes of two hydroxyapatite (HA) ceramics induced by bone ingrowth were in a rabbit model. Doll et al [22] proposed a computational framework to improve the understanding of the mechanical behavior of graphene nanosheet and CNT-reinforced HA-nanocomposites. Paiboon et al [23] investigated the influence of porosity and void size on effective elastic geotechnical engineering properties with a 3D model of random fields and finite element.

The objective of this research is to introduce 3x3x3 cells of porous material that satisfy some conditions. It includes a regular shape with certain dimensional parameters. The porosity contains three elliptical cylinders oriented on three main direction on the reverse of the Cartesian coordinate as in Figure 1. The dimensional parameter is the projection circle radius. By varying the radius, the porosity percentage will change correspondingly. The porosity is the ratio of material solid volume to the total volume. The proposed model should prevent the longitudinal porous cavity by using multidirectional cavities to create obstacle to the crack propagation and to ensure the uniform fluid flow inside the porous cavity material as a web canals.

II. Geometric Modeling

Model includes a regular shape with certain dimensional parameters. The porosity contains three elliptical cylinders oriented on three main direction on the reverse of the Cartesian coordinate as in Figure 1. This model allow any liquid to uniform distribution flow and transmit through the bone bourse media. Different configuration with different orientation of the single model cell will introduce a different collection of models.

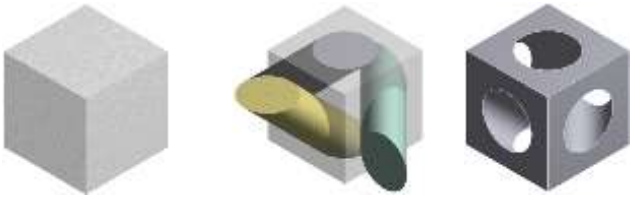

(a) (b) (c)

Figure 1. Cube (a) with cylindrical cavities (b) subtracted through the six faces (c)

3D matrix model has been introducing using single cell joined together to be three cells on three directions. The matrix configuration (arrangement) between cells is side by side. Finite Element methods will utilize to investigate the cells matrix by introducing a fixed lower side and applying a fixed displacement to the upper side as illustrated in Figure 2 (b). The direction of displacement is downward that indicate to compression load. The applied displacement will be used to overcome the elastic region and to take a portion of the plastic region. Thus, we can estimate the elastic modulus and the yield strength for each set. of the cube length. Running the model simulation and calculating the maximum strength intensity factor. Studying the effective of variation of the single cell parameters and the volume ratio with the maximum strength intensity factor using the side-by-side and mirror matrix configurations.

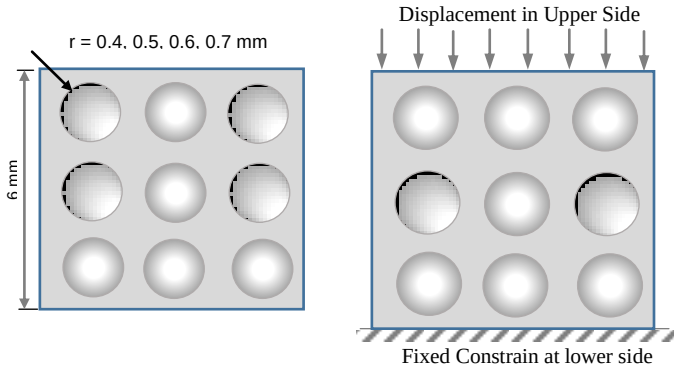

(a) (b)

Figure 2. 2-D views of the 3 x 3 x 3 cells Model showing dimension (a) and constrains (b)

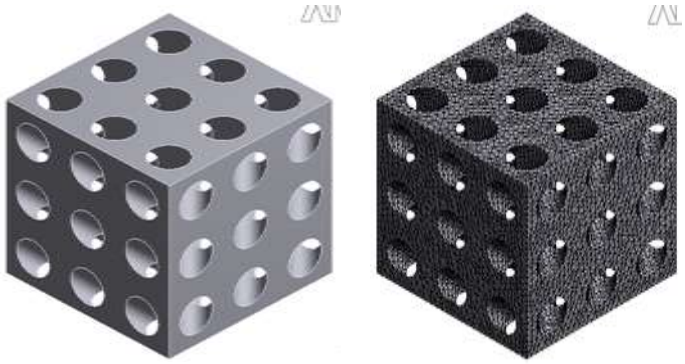

(a) (b)

Figure 3. 3x3x3 Matrix of the single cell to produce 3D cubic porous solid model (a), mesh of the cube matrix (b)

III. Material Modeling

Elastic-plastic properties of CP Ti processed by SLM to characterize the intrinsic properties of CP Titanium processed by SLM, three types of standard tensile test specimens (NF EN ISO 6892-1). The average value of Young's modulus of 100 GPa was deduced from these tests. The commonly admitted value of the Poisson's ratio of 0.33 was also used. The titanium matrix having mechanical properties as shown in Table I. The matrix yield surface follows the Von Mises yield criterion with isotropic hardening. All material properties and model simulations are for room temperature.

The elastic modulus E (MPa) of each model was defined as:

$$E = \frac{\left(\frac{F}{A}\right)}{\left(\frac{\Delta L}{Lo}\right)} = \left(\frac{F}{\Delta L}\right)\left(\frac{Lo}{A}\right) \quad (1)$$

where F (N) is the compressive load, A (mm^2) is the area of loaded surface, ΔL (mm) denotes the amount of deformation, and L_0(mm) is the initial edge length of the cubic model.

TABLE I. TITANIUM BULK MECHANICAL PROPERTIES [5]

Property	Value
Specific Gravity	4.62
Young's Modulus (E) GPa	96
Shear Modulus (G) GPa	35.294
Bulk Modulus GPa	114.29
Poisson's Ratio	0.36
Yield Stress MPa	930
Ultimate Stress MPa	1070

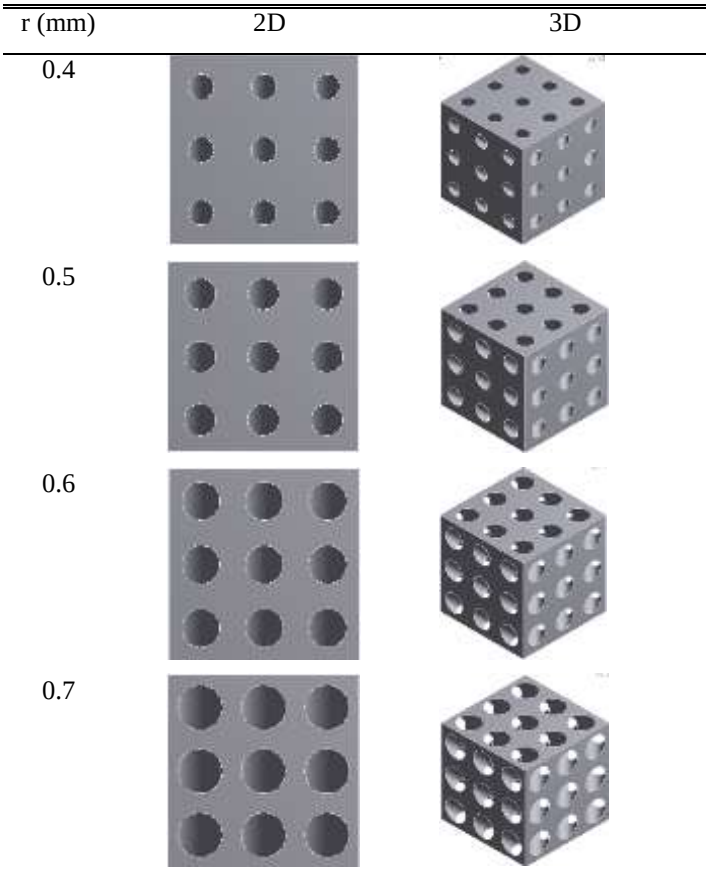

Figure 4. 3x3x3 Matrix with variable projection circle radius from 0.4 mm to 0.7 mm, 2D and 3D models.

$$n\frac{Lo}{A} = constant \quad (2)$$

A= $(Lo)^2$- n (πr^2), where n = number of circles.

Or,

A= $(6)^2$- (9) ($\pi \times 0.4^2$) = 31.48 mm^2; Then, for r = 0.4; Lo/A= 36/31.48= 1.14 mm^{-1}. The amount of deformation ΔL was determined as the average axial displacements of all nodes on the loaded surface. In the first step, the pore size of four FE models in Figure 4 was increased (0.0, 0.4, 0.5, and 0.7 mm) and the resulting scaffold porosity was calculated according to the following equation.

$$\text{Porosity} = (1 - V_e/V_o) \times 100\% \quad (3)$$

where V_o is the overall volume enclosed by the outer periphery (729 mm^3) and V_e is the effective volume of the scaffold struts. The effective volume evaluated using ANSYS software for each cases. That, for (r= 0.4, 0.5, 0.6, 07 mm), the effective volume will be (For example, if the radius is 0.4 then the porosity will be (V_e = 175.29, 152.39, 124.39, 91.31 mm^2). The corresponding porosity are (18.86, 29.45, 42.41, and 57.73).

IV. Results and Discussion

A simple and effective geometric representation for regular porous structure modeling is proposed in this paper. Finite Element simulation has been chosen to study the strength of the bone and to maintain uniform strength along the bone geometry.

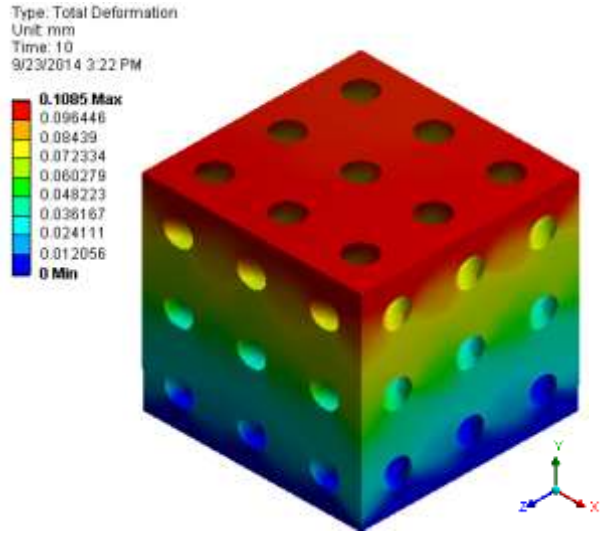

Figure 5. Total displacemnt distripytion of hole radius of 0.4 mm

Compression load was applied to the top surface of the model using gradual displacement downward of the y-axis. The lower surface was fixed from any movement. Displacement range was chosen to grantee the model accomplishing full elastic region end a portion from plastic region.

Figure 5 shows the total defamation distribution on the model at the last stage of compression with 0.4 mm radius corresponding to 18.86 porosity. which appears the maximum displacement was on the top and the minimum at the fixed surface on bottom. Equivalent (Von-Mises) Stress is shown in Figure 6. The minimum is about 100 MPa and the maximum is about 1000 GPa. The maximum equivalent stress supposed to be larger than yield strength because the model was force toward the plastic region as shown in Figure 7. Maximum principle stresses distribution of the model is shown in Figure 7. The minimums was -570 MPa while the Maximum was 825 MPa.

Figure 8 shows the relation between Strain and Stress using porosity of (0, 18.86, 29.45, 42.41, 57.73). The linear relation occurs from 0 to about 0.008 of strain with fixed slope for each porosity.

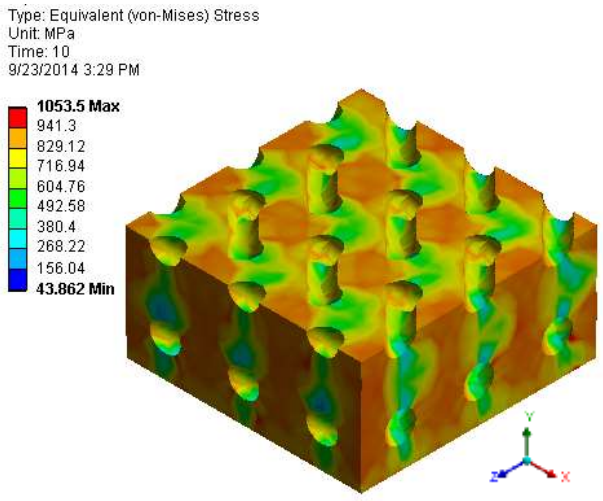

Figure 6. Equivelant Stress distripytion of hole radius of 0.4 mm with cross section on y axix.

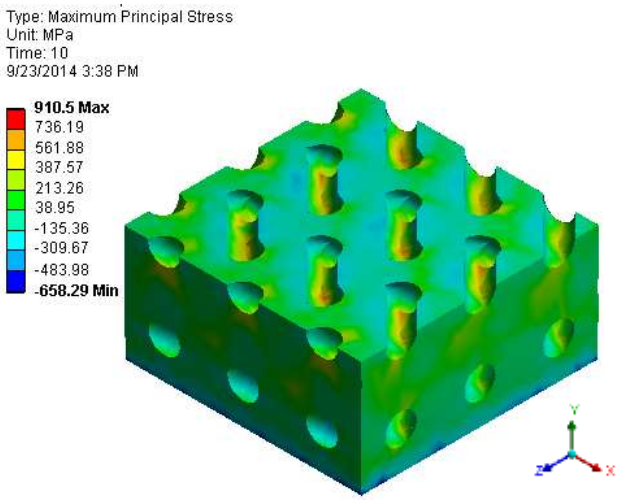

Figure 7. Total displacemnt distripytion of hole radius of 0.4 mm

The elastic modulus *E* was estimated from the slope of the relation between stress and strain at the elastic region and listed in Table II. After that, the slope decreases as the material goes to plastic deformation. The yield strength occupy at the end of elastic region and the start of plastic region. That could be calculate by drawing lane parallel to the curve between stress and strain (Elastic region) and crossing 0.002 of strain at zero stress.

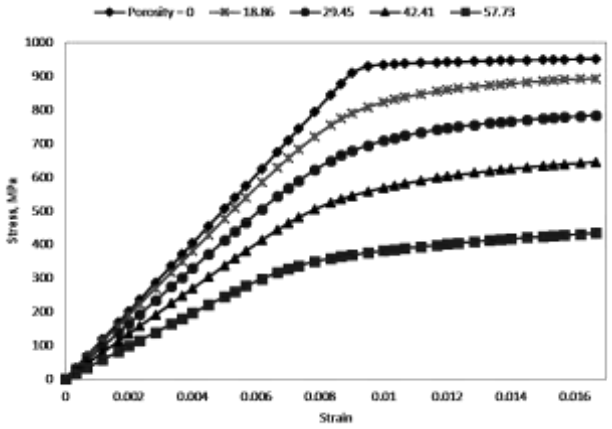

Figure 8. Displacement in y direction vs. reaction force with variation of projection circle radius. (Elastic and Plastic Portions)

TABLE II. TITANIUM BULK MECHANICAL PROPERTIES [5]

r (mm)	Volume mm^3	Porosity %	E (GPa)	Sy (MPa)
0.0	216.00	0	101.13	911.96
0.4	175.29	18.86	74.48	708.36
0.5	152.39	29.45	62.05	585.43
0.6	124.39	42.41	49.45	448.02
0.7	91.311	57.73	35.57	307.29

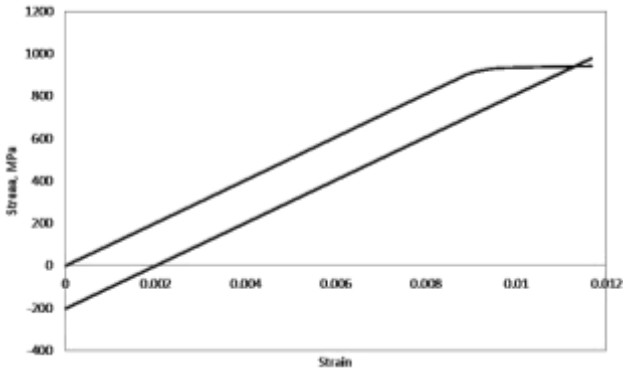

Figure 9. Calculating the Yield Strength by shifting the curve by 0.002

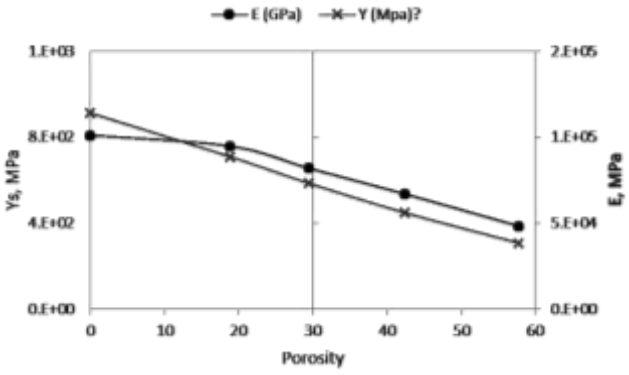

Figure 10. Porosity verse Yield Strength (Left) and Elastic modulus (Right).

The yield strength location will be at the intersection of the line drawn and the stress strain curve at plastic region as in Figure 9. Figure 10 show that inverse linear relation between porosity and yield strength on the left y-axis. The curve fit and the regression R^2 of 0.9984 is shown in equation (4).

$$Sy = -10.567p + 905.95 \quad (4)$$

Simi inverse linear relation also shown for the porosity verse elastic modulus E. The curve fit and the regression R^2 of 0.9515 is shown in equation (4)

$$E = -947.22p + 106723 \quad (5)$$

v. Conclusion

Porosity in bone has many functions that are decreasing the mass of bone relative to its volume, allow fluid to transfer among bones and give some ductility to the bone material. So that, the artificial bone include porosity to imitate bone structure. To achieve the porosity functions on artificial bone many requirement should be consider in addition to the material property and structure requirements. The aim of this paper is to propose some models that satisfy the function of porosity in real bone and attain the requirement on material and structure. Results of the simulation show the model was satisfy the porosity requirements function on the bone.

References

[1] Ram C. Acharya, Sjoerd E.A.T.M. van der Zee, Anton Leijnse, "Porosity–permeability properties generated with a new 2-parameter 3D hydraulic pore-network model for consolidated and unconsolidated porous media", Advances in Water Resources 27 (2004) 707–723.

[2] Craig Schroeder, William C. Regli, Ali Shokoufandeh, Wei Sun, "Computer-aided design of porous artifacts", Computer-Aided Design 37 (2005) 339–353

[3] D. Zeleniakienė, P. Griškevičius, V. Leišis, "The comparative analysis of 2D and 3D microstructural models stresses of porous polymer materials", ISSN 1392 - 1207. MECHANIKA. 2005. Nr.3(53)

[4] V.S. Komlev, F. Peyrin, M. Mastrogiacomo, A. Cedola, A. Papadimitropoulos, F. Rustichelli, R. Cancedda, M.D., "Kinetics of In Vivo Bone Deposition by Bone Marrow Stromal Cells into Porous Calcium Phosphate Scaffolds:An X-Ray Computed Microtomography Study", Tissue Engineering Volume 12, Number 12, 2006, Mary Ann Liebert, Inc.

[5] T. Kujime, M. Tane, S.K. Hyun, H. Nakajima, "Three-dimensional image-based modeling of lotus-type porous carbon steel and simulation of its mechanical behavior by finite element method", Materials Science and Engineering A 460–461 (2007) 220–226.

[6] Jia Ping Li, Pamela Habibovic, Mirella van den Doel, Clayton E. Wilson, Joost R. de Wijn, Clemens A. van Blitterswijk, Klaas de Groot, "Bone ingrowth in porous titanium implants produced by 3D fiber deposition", Biomaterials 28 (2007) 2810–2820

[7] H. Shen, L.C. Brinson,, "Finite element modeling of porous titanium", International Journal of Solids and Structures 44 (2007) 320–335

[8] Benedikt Helgason, F. T., "A modified method for assigning material properties to FE models of bones". Medical Engineering & Physics 30 (2008) 444–453.

[9] S.H. Teoh, C. C., "Bone material properties and fracture analysis: Needle insertion for spinal surgery". Journal of the Mechanical Behavior of Biomedical Materials, 1, (2008) 115–139.

[10] Eduard Verges, Dolors Ayala, Sergi Grau, Dani Tost, "3D reconstruction and quantification of porous structures",Computers & Graphics 32 (2008) 438– 444

[11] X.Y. Kou, S.T. Tan, "A simple and effective geometric representation for irregular porous structure modeling", Computer-Aided Design 42 (2010) 930-941

[12] N. Michailidis, F. Stergioudi, H. Omar, D.N. Tsipas, "An image-based reconstruction of the 3D geometry of an Al open-cell foam and FEM modeling of the material response", Mechanics of Materials 42 (2010) 142–147

[13] N. Michailidis, F. Stergioudi, H. Omar, D. Tsipas, "FEM modeling of the response of porous Al in compression", Computational Materials Science 48 (2010) 282–286

[14] Roman Voronov, Samuel VanGordon, Vassilios I. Sikavitsas, Dimitrios V. Papavassiliou, "Computational modeling of flow-induced shear stresses within 3D salt-leached porous scaffolds imaged via micro-CT", Journal of Biomechanics 43 (2010) 1279–1286

[15] Yan Zaretskiy, Sebastian Geiger, Ken Sorbie, Malte Förster, "Efficient flow and transport simulations in reconstructed 3D pore geometries", Advances in Water Resources 33 (2010) 1508–1516

[16] Su A Park, Su Hee Lee, Wan Doo Kim, "Fabrication of porous polycaprolactone/hydroxyapatite (PCL/HA) blend scaffolds using a 3D plotting system for bone tissue engineering", Bioprocess Biosyst Eng (2011) 34:505–513

[17] L. Podshivalov, A. F.-Y., "3D hierarchical geometric modeling and multiscale FE analysis as a base for individualized medical diagnosis of bone structure", Bone 48 (2011) 693–703

[18] T. Guillén, Q.-H. Z.-J., "Compressive behaviour of bovine cancellous bone and bone analogous materials, microCT characterisation and FE analysis", Journal of the Mechanical Behaviour of Biomedical Materials, (2011), 4, 1452–1461.

[19] Andrea Spaggiari, Noel O'Dowd, Eugenio Dragoni, "Multiscale modelling of porous polymers using a combined finite element and D-optimal design of experiment approach", Computational Materials Science, (2011), 50 2671–2682

[20] Andrea Spaggiari, Noel O'Dowd, "The influence of void morphology and loading conditions on deformation and failure of porous polymers: A combined finite-element and analysis of variance study", Computational Materials Science 64 (2012) 41–46

[21] Li-Mei Ren, M. T. "A comparative biomechanical study of bone ingrowth in two porous hydroxyapatite bioceramics", Applied Surface Science, (2012), 262, 81-88.

[22] Kristopher Doll, Ani Ural, "Mechanical Evaluation of Hydroxyapatite Nanocomposites Using Finite Element Modeling", Journal of Engineering Materials and Technology, January 2013, Vol. 135 / 011007-1

[23] Jumpol Paiboon, D.V. Griffiths, Jinsong Huang, Gordon A. Fenton, "Numerical analysis of effective elastic properties of geomaterials containing voids using 3D random fields and finite elements", International Journal of Solids and Structures 50 (2013) 3233–3241.

About Authors:

Dr. Abdulaziz S. Alaboodi, Associate Professor at Engineering College, Qassim University. Earned his PhD degree in Mechanical Engineering from KFUPM, Saudi Arabia. He had published more than 20 papers in Conferences and Journals.

Eng. Abdulrahman A. Al-Nasser Graduate student at Engineering College at Malay University, Malaysia. And Lecturer at Buraydah College of Technology